RNA (1999), *5*:574–584. Cambridge University Press. Printed in the USA.

Formation of metastable RNA structures by sequential folding during transcription: Time-resolved structural analysis of potato spindle tuber viroid (–)-stranded RNA by temperature-gradient gel electrophoresis

DIRK REPSILBER, SABINE WIESE, MARC RACHEN, ASTRID W. SCHRÖDER, DETLEV RIESNER, and GERHARD STEGER

Institut für Physikalische Biologie, Heinrich-Heine-Universität Düsseldorf, Germany

ABSTRACT

A model of functional elements critical for replication and infectivity of the potato spindle tuber viroid (PSTVd) was proposed earlier: a thermodynamically metastable structure containing a specific hairpin (HP II) in the (–)-strand replication intermediate is essential for template activity during (+)-strand synthesis. We present here a detailed kinetic analysis on how PSTVd (–)-strands fold during synthesis by sequential folding into a variety of metastable structures that rearrange only slowly into the structure distribution of the thermodynamic equilibrium. Synthesis of PSTVd (–)-strands was performed by T7-RNA-polymerase; the rate of synthesis was varied by altering the concentration of nucleoside triphosphates to mimic the in vivo synthesis rate of DNA-dependent RNA polymerase II. With dependence on rate and duration of the synthesis, the structure distributions were analyzed by temperature-gradient gel electrophoresis (TGGE). Metastable structures are generated preferentially at low transcription rates—similar to in vivo rates—or at short transcription times at higher rates. Higher transcription rates or longer transcription times lead to metastable structures in low or undetectable amounts. Instead different structures do gradually appear having a more rod-like shape and higher thermodynamic stability, and the thermodynamically optimal rod-like structure dominates finally. It is concluded that viroids are able to use metastable as well as stable structures for their biological functions.

Keywords: kinetics; rate of transcription; RNA secondary structure; structure formation

INTRODUCTION

Viroids are a class of autonomously replicating subviral pathogens that cause a series of maladies affecting crops and ornamental plants (for reviews see Diener, 1987; Semancik, 1987). They are composed of single-stranded circular RNA in the size range between 245 and 399 nt. Neither the circular RNA nor the complementary (by definition (−)-stranded) RNA code for any protein. Thus viroids may be regarded as minimal parasites of the host. From a functional view, viroids have to present signals to the host to force the transcription and transport machinery of the host to do all necessary actions like replication and transport. These functional signals have to be based only on the RNA, which is the primary sequence as well as the higher structure of viroids.

The following introduction to functions of viroids is based mainly on analysis of potato spindle tuber viroid (PSTVd), which is the type strain of the major viroid group (for classification of viroids see Koltunow & Rezaian, 1989; Flores et al., 1998). The (+)-stranded circular RNA of viroids adopts in its native state a rod-like, highly base-paired structure (for review see Riesner, 1990); it is transcribed by DNA-dependent RNA polymerase II of the host into oligomeric linear (−)-strands (see Fig. 1). The (−)-strands are transcribed again by polymerase II into oligomeric linear (+)-strands (Mühlbach & Sänger, 1979; Schindler & Mühlbach, 1992) that are processed to monomeric units and ligated to circles by host-encoded RNase(s) and ligase(s) (Tsagris et al., 1987). For recognition of the (+)-circular and

Reprint requests to: Dr. Gerhard Steger, Institut für Physikalische Biologie, Geb. 26.12.U1, Heinrich-Heine-Universität Düsseldorf, Universitätsstr. 1, D-40225 Düsseldorf, Germany; e-mail: steger@biophys.uni-duesseldorf.de.

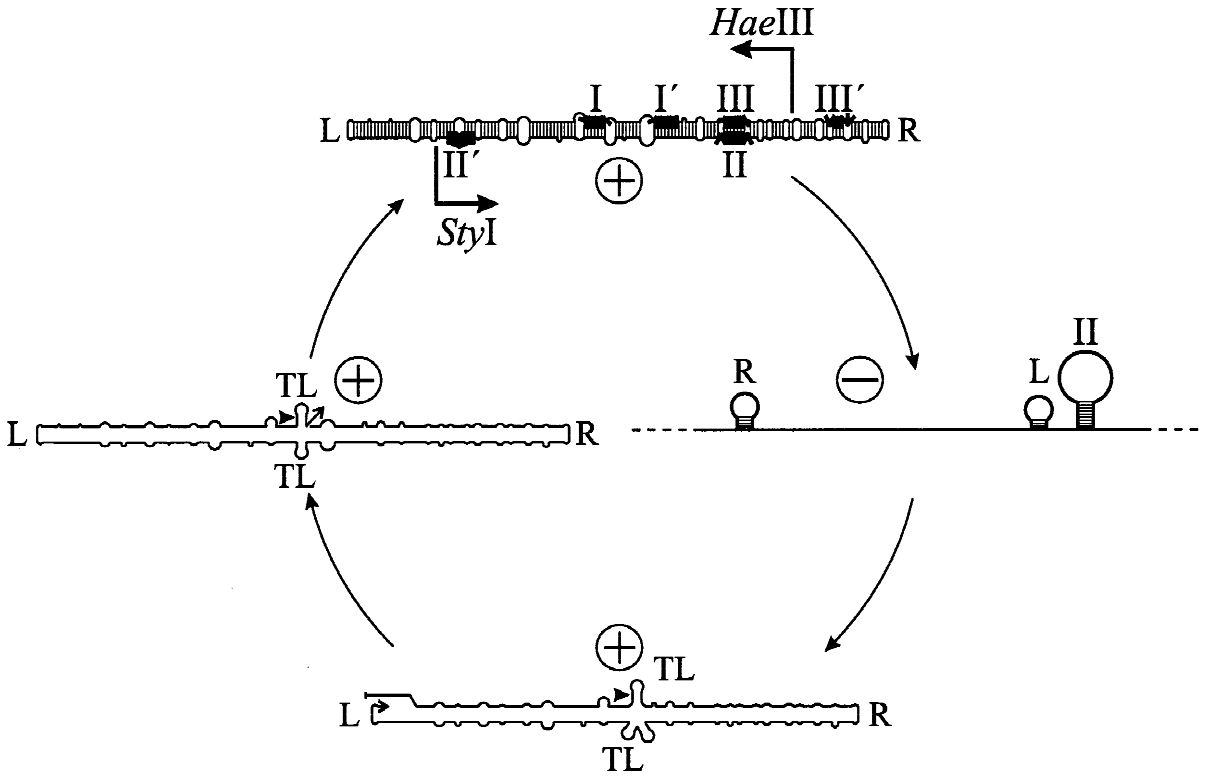

FIGURE 1. Replication cycle of viroids of the PSTVd-class. The mature circular viroid RNA adopts a rod-shaped secondary structure under native conditions (top); during thermal denaturation stable hairpins (I, II, and III) are formed that are not part of the native structure (Henco et al., 1979; Steger et al., 1984). The transcription start sites of the synthetic transcripts PSTVd-*Sty*1 and PSTVd-*Hae*III, used in this work, are marked by appropriately labeled arrows. In vivo transcription by polymerase II and sequential folding during transcription led to (−)-stranded oligomers (right) that are thought to be present in a metastable conformation which includes HP II as an element critical for transcription into (+)-stranded oligomers (Loss et al., 1991) by polymerase II. The (+)-oligomers rearrange into structures with structural termini (L and R) similar to that of the mature circle. In the central part, however, a metastable structure including extrastable tetra-loop hairpins (TL) is formed (Baumstark & Riesner, 1995). This structural part is recognized by host RNase(s) and ligase(s) that process the replication intermediate to circles (left; cleavage and ligation point is marked by a filled triangle; Baumstark et al., 1997), which rearrange easily to the rod-shaped structure (top). Most, if not all, of the mature viroids are located in the nucleoli of infected cells (Harders et al., 1989; Ding et al., 1997).

the (−)-oligomeric RNA as a template by the polymerase II, helical regions with a high G:C content are thought to be responsible. In case of the (+)-circles this helix is part of the thermodynamically optimal secondary structure (Qu et al., 1993; Fels & Riesner, 1998). In the (−)-strand oligomer, a helix called hairpin II (HP II), consisting of nine G:C and one A:U base pairs, is critical for replication (Loss et al., 1991; Qu et al., 1993). However, HP II is present only in metastable structures; that is, HP II-containing structures should not exist under conditions controlled by thermodynamics. As a hypothesis, we assume that such metastable structures containing HP II are formed during synthesis of the RNA because of sequential folding, a term introduced for RNA by Boyle et al. (1980) and Nussinov and Tinoco (1981). After synthesis, the metastable structure should rearrange into a structure of higher thermodynamic stability. This might be impossible, however, because the energetic barrier for rearrangement—dissociation of unfavorable structural elements and formation of more favorable elements—might be too high under in vivo conditions, which would result in a kinetic stabilization of the existing structure(s).

To verify the hypothesis experimentally, we had to rely on in vitro experiments because the concentration of (−)-stranded replication intermediates in planta is very low. Thus we decided to use transcription of PSTVd-cDNA by T7-polymerase as a model system and to adapt that system to natural conditions under three aspects. First, standard conditions for T7 transcription result in a higher transcription rate than is assumed for the natural transcription by polymerase II. Such differences in transcription rate might lead to functional differences in RNA structure (for examples see Lewicki et al., 1993; Chao et al., 1995). To circumvent that problem we varied the transcription rate of T7-polymerase in a wide range by variation of the nucleoside triphosphate (NTP) concentration. Second, the start site of transcription used in vivo is unknown; therefore we used two different plasmids that produce linear

PSTVd RNA with quite different start sites. Third, the analysis of the structure distributions has to be performed depending on time. We used temperature-gradient gel electrophoresis (TGGE; Riesner et al., 1989, 1991) for the detection and characterization of the different RNA structures. As a gel-electrophoretic method, TGGE separates different structures of the same sequence according to their shape; for example, the rod-like, native structure of PSTVd migrates faster than the highly branched, metastable structures. In addition, the temperature dependence of a structure's mobility provides information about the conformational transitions of its structural elements and thus leads to a more precise characterization of the structure. And most important, in the low ionic strength used here for TGGE and at temperatures significantly lower than the transition temperatures of the structures, rearrangement between quite different structures is prevented during the gel run (for review see Riesner et al., 1992; for an example see Baumstark & Riesner, 1995). In summary TGGE allows us to analyze the structure distribution as present at the stop of transcription.

Results obtained with the methodology outlined above support our mechanistic model; that is, PSTVd (−)-stranded RNA folds sequentially during synthesis into metastable structures with high efficiency. Rearrangement of metastable structures into the thermodynamically most stable structure does not reach completion in biologically relevant times. This allows viroids to use a larger number of structures—thermodynamically optimal and metastable ones—for coding of their necessary biological functions.

RESULTS

Analysis of structure distributions by temperature-gradient gel electrophoresis

The two transcripts used in this study, PSTVd-*Sty*1 and PSTVd-*Hae*III, have the sequence of (−)-stranded PSTVd with quite different start sites (see Fig. 1 and Materials and Methods). The 5′ end of PSTVd-*Sty*1 is in the lower left of the rod-shaped structure near the 5′ part of HP II; thus we expect favorable formation of metastable structures containing this extraordinary stable hairpin during synthesis. In contrast, PSTVd-*Hae*III starts in the upper right of the rod-shaped structure far away in sequence from HP II; thus the possibility of metastable structures with HP II should be lower. According to thermodynamic calculations, however, both transcripts should form predominantly a single, rod-shaped secondary structure (see Steger et al., 1986; Hecker et al., 1988); only near the 5′ and 3′ ends small hairpins are formed. This was confirmed experimentally by TGGE analysis of both transcripts (for PSTVd-*Sty*1 see Fig. 2). The equilibrium structure distribution

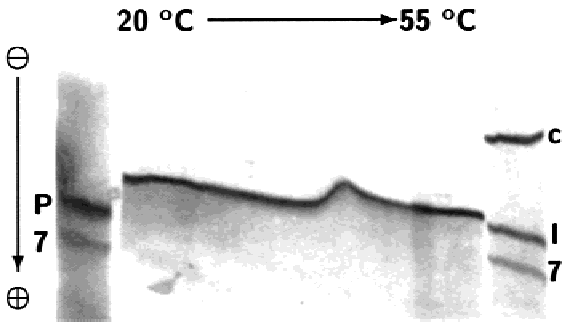

FIGURE 2. TGGE of transcript PSTVd-*Sty*1 under equilibrium conditions. The transcript in 0.2× TBE was denatured at 70 °C for 15 min and slowly renatured to room temperature with ~0.1 °C/min. PAGE: 4% PA 30:1, 0.2× TBE, silver-stained. The marker lanes contain a crude RNA extract with 7: 7 S RNA; P: PSTVd; l: linear PSTVd; c: circular PSTVd. Circular and linear PSTVd comigrate at low temperature because their shape is nearly identical. The completely denatured molecules migrate very differently because of the high retardation of the covalently closed circle.

of the transcripts was established prior to TGGE by slowly cooling the transcripts from the denatured state under low-salt conditions because high-salt conditions would favor dimeric complex formation. Both transcripts are retarded in comparison to circular PSTVd (see low temperature range of Fig. 2). This is due to the few small hairpins at the ends and a sequence length slightly higher than unit length (372 and 369 nt, respectively, versus 359 nt of PSTVd). Near 40 °C the native structure opens up cooperatively under formation of stable hairpins (HP I and HP II), which leads to a slower migration. At still higher temperatures the completely denatured state dominates, which is slightly more retarded than that of linear PSTVd because of its higher length. The relationship between RNA secondary structure and gel mobility has been discussed earlier in reviews on TGGE (see Riesner et al., 1991, 1992); the transition curves measured in this work are in accordance with this relationship. In contrast to the single band observed in TGGE for the RNA under equilibrium conditions, we expect multiple bands for the different metastable states after transcription, which should be (1) of lower thermal stability and (2) of lower mobility, both based on a higher number of small hairpins compared to the thermodynamically optimal state.

Variation of transcription rate

Given optimal conditions for T7-RNA-polymerase, a transcript's chain is elongated with ~230 nt/s at 37 °C (Golomb & Chamberlin, 1974), whereas polymerase II is much slower with ~5–25 nt/s (Kadesch & Chamberlin, 1982; Manley, 1984; Marzluff & Huang, 1984). Assuming that viroids are synthesized with a similar rate by plant polymerase II, we had to decrease the transcription rate of T7-polymerase substantially. This is

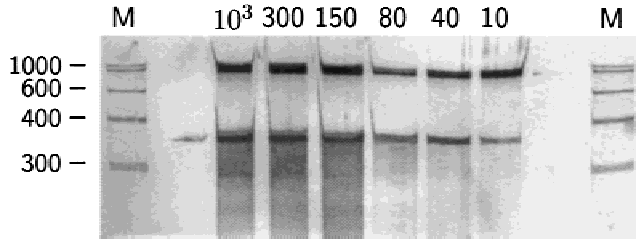

FIGURE 3. Yield and length of transcript PSTVd-*Sty*1 depending on rate of transcription. Transcription assays (50 μL) were stopped after 15 min. Transcripts were purified by phenol/chloroform extraction; 2.5 μL (for c_{NTP} = 1,000–80 μM) or 5 μL (for c_{NTP} = 40–10 μM) per assay were analyzed by PAGE under denaturing conditions. The concentration of NTP is given above the individual lanes in μM. The top band is the DNA template. PAGE: 5% PA 30:1, 8 M urea, 0.5× TBE, 60 °C, silver-stained. Lanes M: length standard (RNA III, Boehringer).

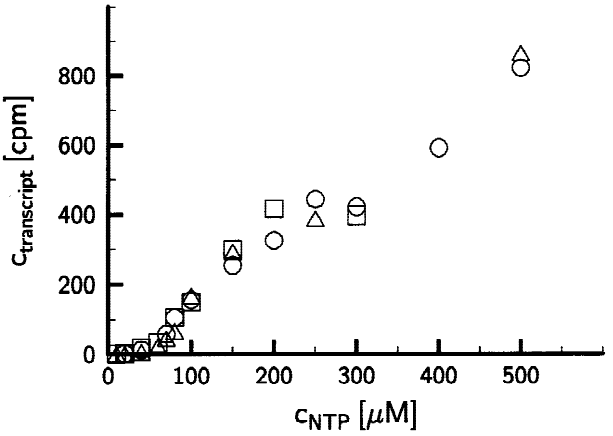

FIGURE 4. Synthesis rate of PSTVd-*Sty*1 depending on concentration of NTP. The different symbols are from independent experiments. After 15 min of transcription with α^{32}P-NTP, transcripts were spotted on Whatman paper, washed with 0.5 M Na_2PO_4, dried, and counted. According to calculations (see text) NTP concentrations of 30 μM and 70 μM are equivalent to transcription rates of ~3 nt/s and ~20 nt/s, respectively. Note the nonlinear dependence of the synthesis rate on the NTP concentration, especially the lag phase at low NTP concentration.

possible through a variety of parameters (temperature, anion concentration, viscosity, specific inhibitors) that, however, also influence RNA structure formation. Therefore, we have chosen to vary the concentration of NTP, which is known to regulate the transcription rate in a wide range (Masukata & Tomizawa, 1990; Chamberlin & Ring, 1973) without altering the RNA structure. All other conditions (see Materials & Methods) were kept constant. For all experiments, the polymerase is used in a 24× molar excess over the template.

Lowering the transcription rate does not lead to an increase in non-full-length transcripts (see Fig. 3). Thus all different bands visible in TGGE will consist of structures with the same sequence and length, differing only in shape. Of course, prematurely terminated transcripts are also generated, but their size heterogeneity will prohibit their detection in gels. Furthermore, the absolute yields of transcript are lowered with decreasing concentrations of NTP, but the total amount of NTPs is not limiting for the yields; after 15 min of transcription the NTP concentration is lowered by less than 5% with all NTP concentrations used.

For determination of transcription rates, the amount of transcripts was determined at 15 min (see Fig. 4); at that time point the rates were influenced neither by a lag phase at short times nor by saturation effects at long times (data not shown). At NTP concentrations below 50 μM a sigmoidal dependence of yields is obvious; this is a well known effect (Chamberlin & Ring, 1973; Kadesch & Chamberlin, 1982). We have no explanation for the step-like dependence near 300 μM NTP. From the concentration dependence of the transcript yields, however, values for the transcription rates can be derived. The value of 230 ± 20 nt/s at c_{NTP} = 400 μM and 37 °C is reduced to ~50 nt/s at 20 °C (Chamberlin & Ring, 1973). Using that value as a basis of calculation, the rates determined here are roughly between 3 nt/s at c_{NTP} = 30 μM and 20 nt/s at c_{NTP} = 70 μM; that is, we are able to shift the transcription rate of the T7-polymerase into the proper range for polymerase II.

According to these rates of transcription, synthesis of a full-length PSTVd transcript needs between a few seconds and several minutes. Because folding of RNA structures (for review see Turner et al., 1990; Riesner & Römer, 1973) requires between microseconds (elongation of helices) and minutes (closure of complex junctions or tertiary foldings), the process of transcription and the process of folding might interfere with each other.

Prior to the detailed analysis of these effects, we checked the yields of full-length transcripts depending on transcription time (see Fig. 5). Again mainly full-length transcripts are produced by T7-polymerase even at the shortest periods of incubation time (30 s); however, the amount of product is very low at these short time points.

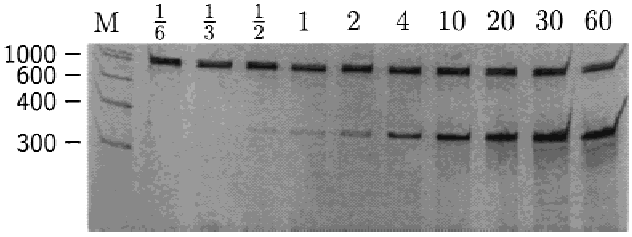

FIGURE 5. Yield and length of transcript PSTVd-*Sty*1 depending on time of transcription. Transcription assays (50 μL with c_{NTP} = 1 mM) were purified by phenol/chloroform extraction; 2.5 μL per assay were analyzed by PAGE under denaturing conditions. The time of transcription is given above the individual lanes in minutes. The top band is the DNA template. PAGE: 5% PA 30:1, 8 M urea, 0.5× TBE, 60 °C, silver-stained. Lane M: length standard (RNA III, Boehringer).

Structure distributions depending on transcription rate

The structure distributions of PSTVd-*Sty*1 were analyzed by TGGE after 15 min of transcription in the presence of different concentrations of NTP. In Figure 6 results are shown for c_{NTP} = 1 mM (top) and c_{NTP} = 30 μM (bottom), which is equivalent to rates of ~130 nt/s and 3 nt/s, respectively. For the high transcription rate the dominant band, labeled S, is equivalent in migration behavior to the single band under equilibrium conditions (see Fig. 2); that is, according to the equilibrium analysis, the structures forming band S will be rod-like near the energetic minimum. All additional bands have to contain metastable structures. The most prominent of these bands is labeled M, and migrates to a position identical to S at low temperature but is retarded prior to the main transition of S. Two additional bands of lower mobility, labeled Q and P, comigrate at low temperature, but separate from each other a few degrees below the main transition of S. A band of very low intensity, labeled R, is visible just above Q/P. All bands comigrate at temperatures above the main transition of S at ~40 °C.

For the low transcription rate, quite different structures do appear (see Fig. 6, bottom). Structures forming a band similar to S are of much lower concentration, whereas at least five additional bands (1 to 5) show up. Because of their slow migration the structures belonging to these bands are at least as branched as those of bands Q, P, and R from the fast transcription. Bands 1 to 5 differ from each other by decreasing mobility and decreasing thermal stability; thus these bands should contain an increasing number of small hairpins and junctions. A band similar to M is hardly visible, and an additional band N seems to approach band S in mobility below the main transition of S. The same band N is visible with the high transcription rate, but only at lower exposure times than shown in Figure 6, top.

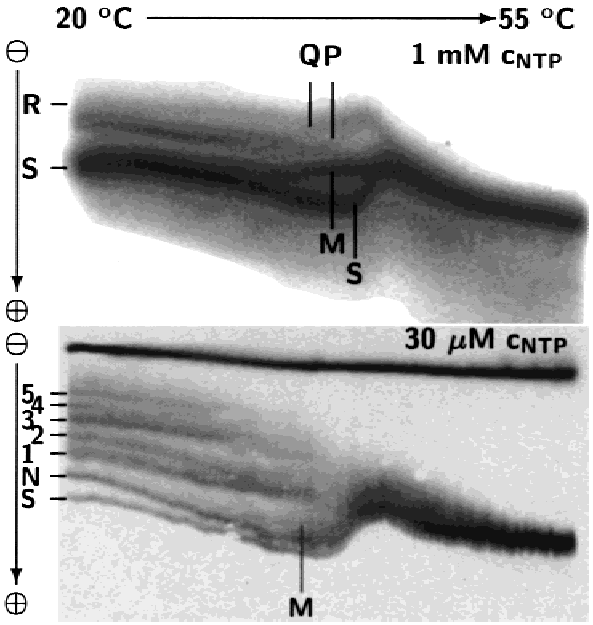

FIGURE 6. TGGE analysis of PSTVd-*Sty*1 depending on transcription rate. Detection of transcripts after 15 min of transcription and TGGE. Top: c_{NTP} = 1 mM, detection by autoradiography. Bottom: c_{NTP} = 30 μM, detection by CDP-*Star*. The most upper band is the DNA template.

To get an impression about the concentrations of the different bands depending on the transcription rate, we quantified the intensity of characteristic bands from native gels at 22 °C by laser densitometry. Results are shown in Figure 7. The relative concentrations of bands S or P/Q increase with increasing transcription rate, which is proportional to the increasing concentrations of NTPs used in the assays. In contrast, the relative concentrations of bands N or 4, which contain metastable structures, decrease. The slopes of these relative concentration changes are, however, quite different: that of band S is steep already at lowest NTP concentrations, whereas those of bands P and Q are ten times less steep. Bands 1–5 decrease about as strongly as band S increases, and are hardly detectable at NTP concentrations above 50 μM. Band N decreases twenty times more slowly, but stays at relatively high concentrations. The concentration of band M could not be evaluated in a similar way because this band was not separated from others at 22 °C.

From the measured concentrations we conclude that structures near the thermodynamic optimum, like those of band S, are easily formed with transcription rates above 20 nt/s; that is, the small hairpins formed during "fast" synthesis do not block the refolding into structures near the thermodynamic optimum after full-length synthesis. Structures of marginal thermodynamic stability, like bands 1 to 5, are formed mainly at lower transcription rates; that is, the small, instable hairpins rearrange prior to full-length synthesis into more complex structures of higher stability, which are too stable to be rearranged into the equilibrium structure of the full-length molecule. This interpretation is extended and specified in Discussion.

Structure distributions depending on transcription duration

The structure distributions of PSTVd-*Sty*1 were analyzed by TGGE at a constant rate of transcription (c_{NTP} = 1 mM; ~130 nt/s) depending on time of transcription. In Figure 8 results are shown for 1 h (top) and 30 s (bottom) transcription time. With c_{NTP} = 1 mM, results at 1 h transcription time are nearly identical to that at 15 min (compare top parts of Figs. 8 and 6). Surprisingly, for short times the results with high-rate transcription are also similar to those with low-rate transcription (compare bottom parts of Figs. 8 and 6); that is, bands S, M, and N are comparable in concentration

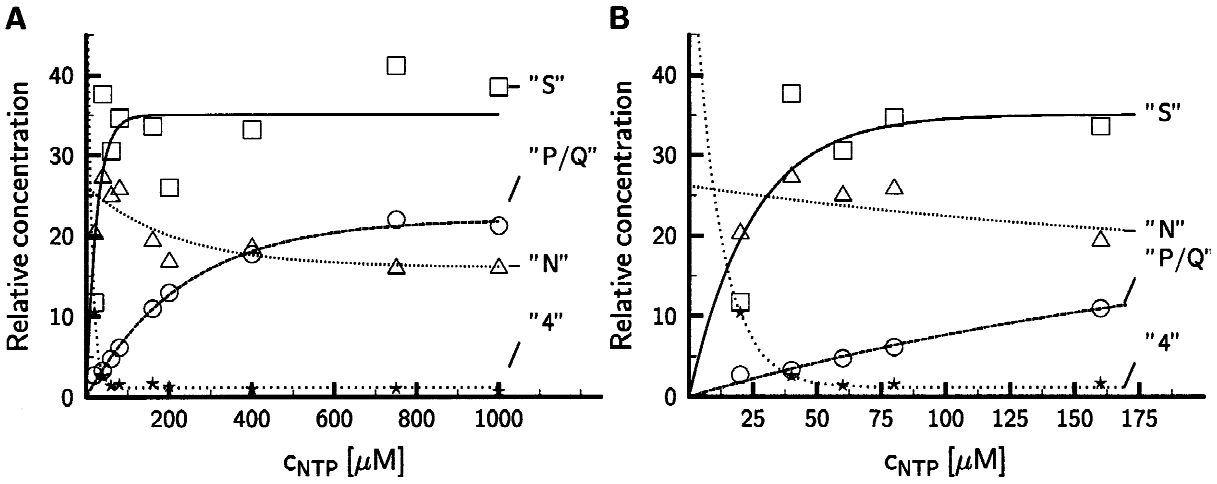

FIGURE 7. Relative concentrations of certain PSTVd-*Sty*1-structures depending on transcription rate. **B** shows an enlarged graph of **A** to allow for visualization of data points at low NTP concentrations. PSTVd-*Sty*1 was synthesized for 15 min in the presence of varying concentrations of NTP; for conversion into transcription rate, see Figure 4. Reactions were stopped with stop buffer and products separated by native PAGE at 22 °C (4% PA 30:1, 0.2× TBE). Bands were quantified by laser densitometry of their CDP-*Star*-luminescence signals on X-ray film. For each NTP concentration the sum of all signals was set to 100%. For designation of bands or structures see Figure 6 and text. The lines connecting the data points are fits to appropriate exponentials.

to at least five different bands containing branched structures of lower thermal stability.

The amounts of bands or structures depending on time of transcription are shown in detail in Figure 9. Structures of band S, which are similar to the thermodynamically most stable rod-like secondary structure, increase in concentration nearly linearly with time after a lag phase of ~2 min; during the time course the concentration of band S does not reach a plateau value. Structures of band M behave very similarly (the concentration of M was determined at ~35 °C where M is well separated from S). Band N also increases steeply but reaches a plateau. Bands a–e containing metastable structures reach a steady-state level at very low concentrations after ~2 min. The nomenclature of the bands was choosen as follows: bands are labeled with capital letters if present in gels with any transcription rate and any incubation time; we are quite sure that bands with identical labels contain identical structures because migration distances and denaturation behavior agree. Bands labeled with small letters or numbers appear only at low transcription rates or at low transcription times, respectively; we are not sure that these bands, for example 1 and a, contain identical structures because of small but noticeable differences in their behavior.

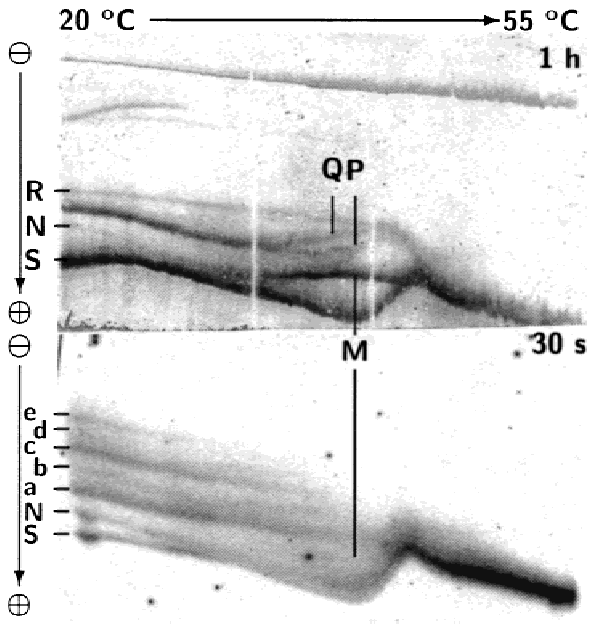

FIGURE 8. TGGE analysis of PSTVd-*Sty*1 after different times of transcription and incubation. Transcription assays with c_{NTP} = 1 mM were stopped with stop buffer after 1 h (top) or after 30 s (bottom). Detection of transcripts by staining with NBT/BCIP (top) or by autoradiography (bottom). In the top gel the most upper band is the DNA template.

For the PSTVd-*Hae*III transcript, structures depending on time appear (Fig. 10) that are quite different from those of the PSTVd-*Sty*1 transcript (Fig. 8). For short transcription times only two bands are visible (Fig. 10, bottom). The band of highest mobility is identical in migration to the band under equilibrium conditions (data not shown); to differentiate it from the S-band of PSTVd-*Sty*1, it is called S*. Band S* is relatively broad; sometimes a further band seems to migrate just above the main band. The second band, called W, is of similar concentration as S* but its structures clearly have to be much bulkier than that of S*.

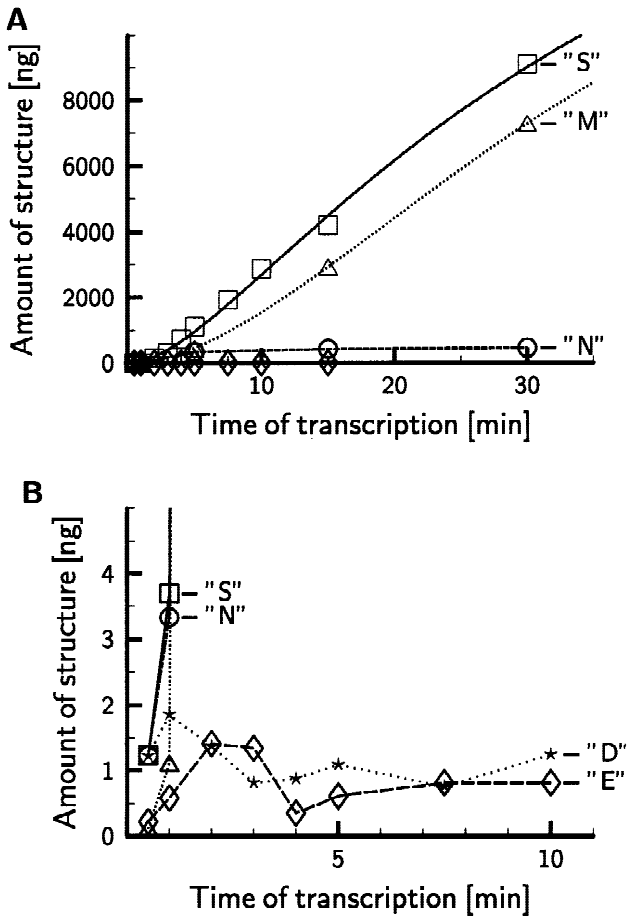

FIGURE 9. Amount of certain PSTVd-*Sty*1 structures depending on time of transcription. Transcription assays with c_{NTP} = 1 mM were stopped with stop buffer after different periods of time. Transcripts were separated by native PAGE at 22 °C or by TGGE. Bands were quantified by laser densitometry of the gel at 22 °C or of the TGG at ~35 °C, where M is well separated from S. **B** shows an enlarged graph of **A** to allow for visualization of structures present only in low concentrations. For designation of bands or structures see Figure 8 and text. The lines connecting data points for structures S and M are fits according to $s = n_0[1 - (k_4/(k_4 - k_1))e^{-k_1 t} + (k_1/(k_4 - k_1))e^{-k_4 t}]$, which is based on the consecutive reactions NTP $\xrightarrow{k_1}$ X $\xrightarrow{k_4}$ S with a metastable structure X and an optimal structure S.

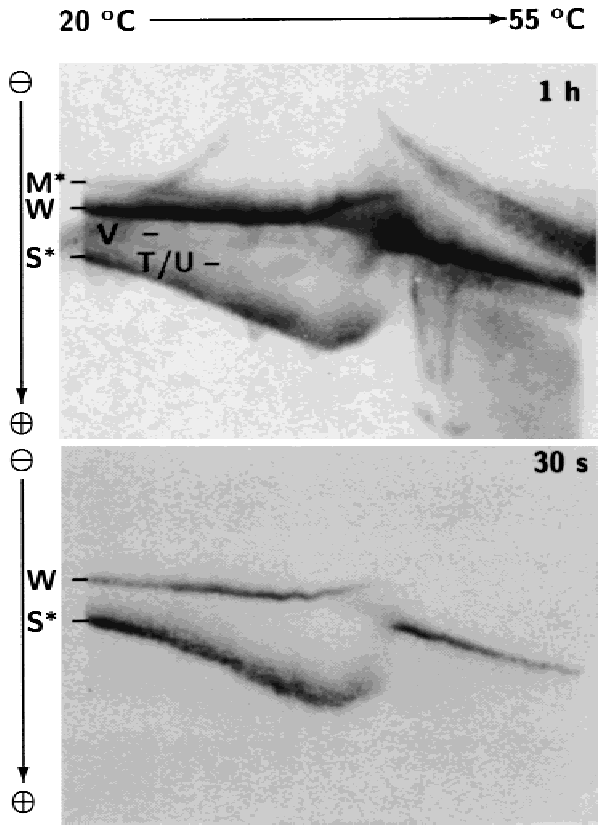

FIGURE 10. TGGE analysis of PSTVd-*Hae*III after different times of transcription and incubation. Transcription assays with c_{NTP} = 1 mM were stopped with stop buffer after 1 h (top) or after 30 s (bottom). Detection of transcripts by CDP-*Star*.

With increasing time of transcription, additional bands appear (Fig. 10, top). Bands T, U, and V are of low concentration even after 1 h of transcription. T and U comigrate at 25 °C but separate from each other at 35 °C; T approaches the migration of V, a band just above T and U at 25 °C, prior to complete denaturation at ~42 °C whereas U decreases continuously in migration. Band M* increases continuously in mobility and shows no significant alteration in mobility near the main transition of S*.

DISCUSSION

We analyzed the formation of structure distributions for PSTVd (−)-stranded RNAs depending on transcription rate and on time of incubation under transcription conditions. For separation and analysis of structures we used TGGE; thus we will discuss first advantages and limitations of that method and then draw conclusions from the results.

One should note that in most experiments the duration of the transcription assay is in fact a summation of two phases, the transcription process and the consecutive incubation in the high-salt transcription buffer. The second phase is longest for those molecules synthesized during the first round of transcription. Only in experiments in which the synthesis takes nearly the whole time of the transcription assay are all molecules fairly synchronized with respect to rearrangements into more stable structures.

Analysis of structure distributions by TGGE

We resolved by TGGE the different structures of transcripts after in vitro synthesis. All bands visible in gels after staining contain full-length transcripts, because the size heterogeneity of non-full-length molecules will lead only to some background smear. Certainly several bands contain more than one structure; for example,

in Figures 6 and 8, M comigrates with S at low temperatures, or Q and P separate from each other prior to complete denaturation. These comigrating structures differ most probably by small structural variations only, so that their "electrophoretic" shapes coincide in a certain temperature range, but after partial denaturation, which happens at different temperatures because of the different structural elements, different electrophoretic mobilities are generated. Even if a band stays as a single band over the whole temperature range, we cannot conclude that it contains only a single structure: first, different structures that interchange rapidly in the TGGE-buffer show up as a single band of intermediate mobility, and second, not each structural difference leads to a difference in electrophoretic mobility.

The discussion above corresponds with our failure to detect defined structures by chemical mapping in most bands; that is, both types of bands—those containing rapidly interconverting structures and those containing more than one structure—will not lead to interpretable mapping signals. However, that failure might also be a consequence of the high degree of base pairing in viroid structures independent from the overall base pairing scheme and stability of the respective structure(s); that is, for quite different structures viroids use different combinations from the same pool of subsequences for pairing.

Metastable structures of PSTVd transcription intermediates

The TGGE analysis of PSTVd-*Sty*1 shows that the highest number of different bands appears for low transcription rates at intermediate transcription assay times or short transcription assay times at high transcription rates. In both cases little time is left over for incubation after completing the synthesis of the RNA. Most of these bands (e.g., bands 1–5 of Fig. 6 and a–e of Fig. 8) might be characterized as containing highly metastable structures by the following criteria: (1) The structures migrate slowly in TGGE; that is, they have a degree of friction higher than the thermodynamic optimal structure. This points to structures with an increasing number of junctions and consequently small hairpins or stem-loop structures. (2) With increasing retardation—following series 1–5 or a–e—the bands vanish at decreasing temperatures in TGGE; that is, the structures either rearrange irreversibly into structures of higher thermodynamic stability or denature more easily. This effect points again to structures with an increasing number of junctions and small stem-loop structures. With increasing transcription rates or increasing transcription/incubation times, these highly metastable structures approach the detection limit or are undetectable. Instead different structures do appear that are less retarded and have higher thermodynamic stability, and the thermodynamically optimal structure becomes the structure of highest concentration.

This behavior is as expected if one takes into account consecutive reactions for structure formation in parallel, for example, those as follow:

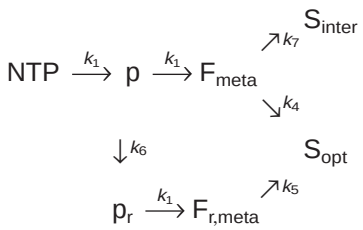

NTP denotes an unlimited supply for production of transcripts. The polymerase synthesizes partial transcripts p that fold into different structures depending on their length: (1) If synthesis is fast only small hairpins are formed and the resulting full-length transcript F_{meta} is also highly metastable. (2) If synthesis is slow the partial transcript p has sufficient time to rearrange into p_r, for example by formation of junctions, and the resulting full-length transcripts $F_{r,meta}$ have structures of higher stability. These consequences follow quite easily from the known rates of synthesis and RNA structure formation (for review see Turner et al., 1990; Riesner & Römer, 1973), respectively. For example, the relaxation times for formation of small hairpin loops at room temperature are in the microsecond range, whereas relaxation times of clover leaf formation are in the range of seconds.

After synthesis the various metastable structures (F_{meta} and $F_{r,meta}$) can rearrange into structures of higher thermodynamic stability. As an example, F_{meta} might rearrange into the thermodynamic optimum S_{opt} but also into a structure S_{inter} of intermediate stability; the metastable structure $F_{r,meta}$ can also rearrange into the optimal structure S_{opt} but with a higher activation energy. A rearrangement of $F_{r,meta}$ into a structure similar to S_{inter} should also be possible, but is not introduced here into the reaction scheme because of the higher stability of $F_{r,meta}$ in comparison to F_{meta}. Resulting concentrations for the various structures as calculated by *KinSim* (Barshop et al., 1983; Dang & Frieden, 1997; *KinSim*, 1998) are shown in Figure 11. The rate constants (in arbitrary units) used for calculations are (1) $k_1 = 1.0$ or 0.08, the first implying fast and the second slow transcription. (2) $k_4 = 1.0$, which is at least as fast as the synthesis steps resulting in a high concentration of transcripts S_{opt} with optimal structures and very low concentrations of their metastable precursors F_{meta}. (3) $k_7 = 0.5$ allows for formation of a quite stable but nevertheless metastable structure S_{inter} in parallel to formation of the optimal structure S_{opt} out of the metastable precursors F_{meta}. (4) $k_5 = 0.1$, which is slower than k_4, resulting in accumulation of the metastable precursor $F_{r,meta}$; that is, rearrangement from $F_{r,meta}$ into the opti-

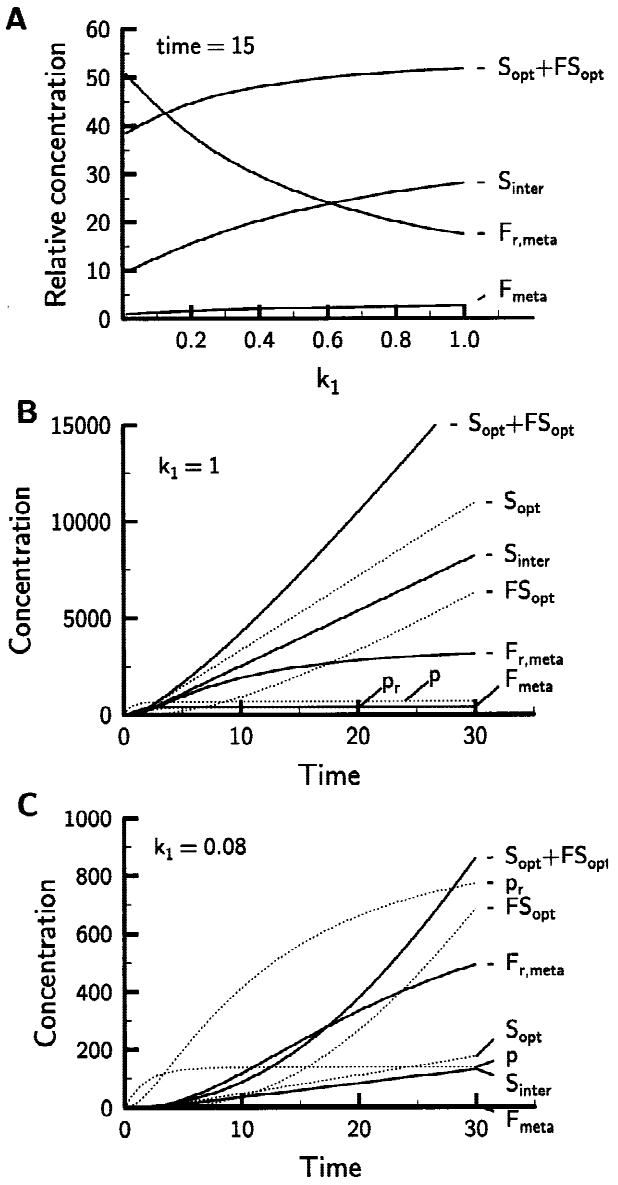

FIGURE 11. Simulation of structure formation. Simulations were performed according to the chemical equations NTP $\xrightarrow{k_1}$ p $\xrightarrow{k_1}$ F_{meta} $\xrightarrow{k_4}$ S_{opt}, F_{meta} $\xrightarrow{k_7}$ S_{inter}, p_r $\xrightarrow{k_1}$ $F_{r,meta}$ $\xrightarrow{k_5}$ FS_{opt}, p $\xrightarrow{k_6}$ p_r. The initial concentration of NTP was held constant during reaction time. Partial transcript p might stabilize its structure to p_r by refolding; both are transcribed into full-length molecules F_{meta} and $F_{r,meta}$ with different but highly metastable structures. F_{meta} is allowed to rearrange into S_{inter} and the optimal structure S_{opt}, whereas $F_{r,meta}$ rearranges more slowly into the identical structure S_{opt}, which is named FS_{opt} only as a reference to its precursor. Rate constants and times are given in arbitrary units. The rate constants were $k_1 = 1$ (middle) and 0.08 (bottom), respectively, $k_4 = 1$, $k_5 = 0.1$, $k_6 = 0.5$, and $k_7 = 0.5$. Curves of full-length, observable transcripts are given by thick lines; those of incomplete transcripts by dotted lines. For further details see text.

mal structures S_{opt} is kinetically blocked in comparison to the rearrangement of F_{meta} into S_{opt}. (5) $k_6 = 0.5$ gives rise to the two major parallel pathways; its value in relation to that of the synthesis steps (k_1) determines the relative population of both pathways.

Figure 11A might be compared qualitatively with Figure 7. Obviously the relative concentrations of structures in dependence upon transcription rate are modeled adequately; that is, the optimal structure S_{opt} changes only slightly in relative concentration when the transcription rate is changed by orders of magnitude; the relative concentration of metastable structures P/Q and S_{inter} increases more than that of the optimal structure; and the relative concentration of the metastable structure N and $F_{r,meta}$, respectively, drops significantly. Next we compare Figure 11B with Figure 9A. The time dependence of the experimentally determined amount of structures migrating in band S is in accordance with the total concentration of structure S_{opt}, M is in accordance with the metastable structure S_{inter}, and d and e are similar to the highly metastable structures $F_{r,meta}$ and F_{meta}. From comparison of Figure 11C with Figure 6, bottom, the change in proportion of stable to metastable structures (S to, for example, 1 and S_{opt} to $F_{r,meta}$, respectively) is also modeled quite correctly. In total these comparisons suggest that the simple model of consecutive reactions in parallel fits the experimental results.

CONCLUSIONS

We analyzed the structure formation of PSTVd (−)-stranded RNAs in vitro after synthesis by T7-polymerase. The in vitro synthesis rate, which influences the RNA structure formation, was lowered to rates comparable to those probably used in vivo by polymerase II. As shown by the TGGE analysis, the PSTVd (−)-transcripts easily form a variety of metastable structures due to sequential folding when the transcription rate is slowed down to the proper rate of a few nucleotides per second. With increasing time of incubation in the transcription buffer, the metastable structures rearrange into structures of higher thermodynamic stability. The equilibrium structure distribution is only reached by a denaturation/renaturation cycle in practicable times (compare with results from slow temperature-jump experiments for (+)-stranded circular PSTVd; Henco et al., 1977). In view of the in vivo situation, the results are quite obvious for viroids' replication cycle: the transcription rate of polymerase II, which is relatively low in comparison to folding times of simple stem-loop structures, is the basis for the appearance of viroids' (−)-stranded replication intermediates in metastable structures.

However, several open questions remain. For example, does the (unknown) start site(s) of transcription used in vivo have a major influence on the number and concentration of metastable structures? Which of the metastable structures contains the structural element HP II, which was derived earlier from molecular-biological experiments (Loss et al., 1991; Qu et al., 1993) as essential for viroid replication?

MATERIALS AND METHODS

Templates for transcription

Two plasmids, pSH1 and pRH716, were used as templates for transcription with T7-RNA polymerase. pSH1 and pRH716 are derivatives of pRH701 (Hecker et al., 1988). After restriction with either *Sty*1 or *Hae*III, the sense DNA of PSTVd strain Intermediate (Di) was cloned into the multicloning site of pRH701. After linearization with *Eco*RI, run-off transcription with T7-RNA-polymerase results in either a 372-nt transcript with sequence 5′-GGCAAG—(−)PSTVd Intermediate (Di) (337-1/359-338)—GGGAAUU-3′, called PSTVd-*Sty*1, or a 368-nt transcript with sequence 5′-GG—(−)PSTVd Intermediate (Di) (146-1/359-146)—GGGAAUU-3′, called PSTVd-*Hae*III. The numbering of the PSTVd sequence is according to Gross et al. (1978).

T7-RNA-polymerase transcription

T7 run-off transcriptions were performed as described (Davanloo et al., 1984; Hecker et al., 1988) at 25 °C with 1 U/μL RNAsin (Pharmacia) and 6 U/mL T7-RNA-polymerase in a 50 μL assay. Concentrations of all four NTP were varied to obtain different transcription rates (see Results and Fig. 4). Transcription was stopped by lowering salt concentration and complexing Mg^{2+} adding 150 μL (3 volumes) of stop buffer (9 mM Tris/borate, pH 8.3, 5 mM EDTA). To obtain radioactively labeled transcripts, α^{32}P-UTP was used in the transcription assay, but the end concentration of UTP was adjusted to those of the three other NTP. For this reason the rate of incorporation was low in comparison with standard radiolabeling procedures.

Temperature-gradient gel electrophoresis

Structure distributions after transcription were characterized by TGGE (Rosenbaum & Riesner, 1987). Perpendicular to the direction of electrophoresis a linear temperature gradient between 20 °C and 55 °C was established, resulting in the separation of different secondary structures of the transcripts. The polyacrylamide gel [4% polyacrylamide 30:1, 0.2× TBE (1× TBE is 89 mM Tris, 89 mM borate, pH 8.4, 2.5 mM EDTA), 0.2% TEMED (N,N,N′,N′-tetramethylethylendiamine), 0.04% ammoniumperoxodisulfate, 0.2 mm thick] polymerized for 1 h. Electrophoresis of samples was performed in three steps: (1) electrophoresis for 15 min with 30 V/cm at a constant temperature of 15 °C, (2) establishment of the temperature gradient, and (3) electrophoresis for 2 h at 30 V/cm.

Detection of transcription products

After gel electrophoresis transcripts were detected by silver staining (Schumacher et al., 1983), by autoradiography on X-OMAT AR (Kodak), or by electroblotting and nonradioactive hybridization using a digoxigenin-labeled probe (Beuther et al., 1992) followed by either immunodetection with CDP-**Star**™ (Boehringer Mannheim) as chemiluminescence or colorimetry with NBT/BCIP (Boehringer Mannheim). The digoxigenin-probe was synthesized by transcription of pRH713 (see Hecker et al., 1988) with DIG-11-dUTP (Boehringer Mannheim) in the transcription assay, resulting in a labeled transcript with dimeric (+)-strand sequence of PSTVd Intermediate (Di).

For quantification of transcription products, transcripts were radiolabeled with α^{32}P-dUTP, spotted on DE81 Whatman paper, washed 2 times with 0.5 M Na_2HPO_4, dried, and counted in 5 mL of scintillation solution.

For quantification of autoradiographs of radiolabeled transcripts or CDP-*Star*-luminescence signals, bands were scanned with a laser densitometer (Personal Densitometer SI, Molecular Dynamics). For quantitative performance of blotting and nonradioactive detection several exposures of one gel were used so as not to leave the linear range of detection.

ACKNOWLEDGMENTS

We thank Drs. T. Baumstark, K. Buschmann, A. Fels, M. Schmitz, and U. Wiese for their support and stimulating discussions throughout this work. This work was supported by grants to D.R. and G.S. from the Deutsche Forschungsgemeinschaft and Fonds der Chemischen Industrie.

Received November 11, 1998; returned for revision December 4, 1998; revised manuscript received December 24, 1998

REFERENCES

Barshop BA, Wrenn RF, Frieden C. 1983. Analysis of numerical methods for computer simulation of kinetic processes: development of KINSIM—a flexible, portable system. *Anal Biochem 130*:134–145.

Baumstark T, Riesner D. 1995. Only one of four possible secondary structures of the central conserved region of potato spindle tuber viroid is a substrate for processing in a potato nuclear extract. *Nucleic Acids Res 23*:4246–4254.

Baumstark T, Schröder AR, Riesner D. 1997. Viroid processing: Switch from cleavage to ligation is driven by a change from a tetraloop to a loop E conformation. *EMBO J 16*:599–610.

Beuther E, Wiese U, Lukács N, van Slobbe WG, Riesner D. 1992. Fatal yellowing of oil palms: Search for viroids and double-stranded RNA. *J Phytopath 136*:297–311.

Boyle J, Robillard GT, Kim SH. 1980. Sequential folding of transfer RNA: A nuclear magnetic resonance study of successively longer tRNA fragments with a common 5′ end. *J Mol Biol 139*:601–625.

Chamberlin M, Ring J. 1973. Characterization of T7-specific ribonucleic acid polymerase. I. General properties of the enzymatic reaction and the template specificity of the enzyme. *J Biol Chem 248*:2235–2244.

Chao MY, Kan MC, Lin-Chao S. 1995. RNAII transcribed by IPTG-induced T7 RNA polymerase is non-functional as a replication primer for ColE1-type plasmids in *Escherichia coli. Nucleic Acids Res 23*:1691–1695.

Dang Q, Frieden C. 1997. New PC versions of the kinetic-simulation and fitting programs, KINSIM and FITSIM. *Trends Biochem Sci 22*:317.

Davanloo P, Rosenberg AH, Dunn JJ, Studier FW. 1984. Cloning and expression of the gene for bacteriophage T7 RNA polymerase. *Proc Natl Acad Sci USA 81*:2035–2039.

Diener TO, ed. 1987. *The viroids.* New York: Plenum Press.

Ding B, Kwon MO, Hammond R, Owens R. 1997. Cell-to-cell movement of potato spindle tuber viroid. *Plant J 12*:931–936.

Fels A, Riesner D. 1998. Transcription start sites in potato spindle tuber viroid. Submitted.

Flores R, Randles JW, Bar-Joseph M, Diener TO. 1998. A proposed scheme for viroid classification and nomenclature. *Arch Virol 143*:623–629.

Golomb M, Chamberlin M. 1974. Characterization of T7-specific ribonucleic acid polymerase. IV. Resolution of the major in vitro transcripts by gel electrophoresis. *J Biol Chem 249*:2858–2863.

Gross HJ, Domdey H, Lossow C, Jank P, Raba M, Alberty H, Sänger HL. 1978. Nucleotide sequence and secondary structure of potato spindle tuber viroid. *Nature 273*:203–208.

Harders J, Lukács N, Robert-Nicoud M, Jovin TM, Riesner D. 1989. Imaging of viroids *in nuclei* from tomato leaf tissue by *in situ* hybridization and confocal laser scanning microscopy. *EMBO J 8*:3941–3949.

Hecker R, Wang Z, Steger G, Riesner D. 1988. Analysis of RNA structure by temperature-gradient gel electrophoresis: Viroid replication and processing. *Gene 72*:59–74.

Henco K, Riesner D, Sänger HL. 1977. Conformation of viroids. *Nucleic Acids Res 4*:177–194.

Henco K, Sänger HL, Riesner D. 1979. Fine structure melting of viroids as studied by kinetic methods. *Nucleic Acids Res 6*:3041–3059.

Kadesch TR, Chamberlin MJ. 1982. Studies of in vitro transcription by calf thymus RNA polymerase II using a novel duplex DNA template. *J Biol Chem 257*:5286–5295.

KinSim. 1998. For obtaining the program see: http://www.biochem.wustl.edu/cflab/, http://unix.hensa.ac.uk/cgi-bin/cftp/wuarchive.wustl.edu/packages/kinsim and ftp://wuarchive.wustl.edu/packages/kinsim.

Koltunow AM, Rezaian MA. 1989. A scheme for viroid classification. *Intervirology 30*:194–201.

Lewicki BT, Margus T, Remme J, Nierhaus KH. 1993. Coupling of rRNA transcription and ribosomal assembly in vivo. Formation of active ribosomal subunits in *Escherichia coli* requires transcription of rRNA genes by host RNA polymerase which cannot be replaced by bacteriophage T7 RNA polymerase. *J Mol Biol 231*:581–593.

Loss P, Schmitz M, Steger G, Riesner D. 1991. Formation of a thermodynamically metastable structure containing hairpin II is critical for infectivity of potato spindle tuber viroid RNA. *EMBO J 10*:719–727.

Manley JL. 1984. Transcription of eukaryotic genes in a whole-cell extract. In: Hames BD, Higgins SJ, eds. *Transcription and translation—a practical approach*. Oxford, UK, Washington, DC: IRL Press. pp 71–88.

Marzluff WF, Huang RCC. 1984. Transcription of RNA in isolated nuclei. In: Hames BD, Higgins SJ, eds. *Transcription and translation—a practical approach*. Oxford, UK, Washington, DC: IRL Press. pp 89–129.

Masukata H, Tomizawa J. 1990. A mechanism of formation of a persistent hybrid between elongating RNA and template DNA. *Cell 62*:331–338.

Mühlbach HP, Sänger HL. 1979. Viroid replication is inhibited by α-amanitin. *Nature 278*:185–188.

Nussinov R, Tinoco I Jr. 1981. Sequential folding of a messenger RNA molecule. *J Mol Biol 151*:519–533.

Qu F, Heinrich C, Loss P, Steger G, Tien P, Riesner D. 1993. Multiple pathways of reversion in viroids for conservation of structural elements. *EMBO J 12*:2129–2139.

Riesner D. 1990. Structure of viroids and their replication intermediates: Are thermodynamic domains also functional domains? *Sem Virol 1*:83–99.

Riesner D, Baumstark T, Qu F, Klahn T, Loss P, Rosenbaum V, Schmitz M, Steger G. 1992. Physical basis and biological examples of metastable RNA structures. In: Lilley D, Heumann H, Suck D, eds. *Structural tools for the analysis of protein-nucleic acid complexes. Advances in life sciences*. Basel, Switzerland: Birkhäuser Verlag AG. pp 401–435.

Riesner D, Henco K, Steger G. 1991. Temperature-gradient gel electrophoresis: A method for the analysis of conformational transitions and mutations in nucleic acids and proteins. In: Chrambach A, Dunn MJ, Radola BJ, ed. *Advances in electrophoresis. Vol. 4.* Weinheim, Germany: VCH Verlagsgesellschaft. pp 169–250.

Riesner D, Römer R. 1973. Thermodynamics and kinetics of conformational transitions in oligonucleotides and tRNA. In: Duchesne J, ed. *Physico-chemical properties of nucleic acids, Vol. 2: Structural studies on nucleic acids and other biopolymers*. London, New York: Academic Press. pp 237–317.

Riesner D, Steger G, Zimmat R, Owens RA, Wagenhöfer M, Hillen W, Vollbach S, Henco K. 1989. Temperature-gradient gel electrophoresis: Analysis of conformational transitions, sequence variations, and protein-nucleic acid interactions. *Electrophoresis 10*:377–389.

Rosenbaum V, Riesner D. 1987. Temperature-gradient gel electrophoresis. Thermodynamic analysis of nucleic acids and proteins in purified form and in cellular extracts. *Biophys Chem 26*:235–246.

Schindler IM, Mühlbach HP. 1992. Involvement of nuclear DNA-dependent RNA polymerases in potato spindle tuber viroid replication: A reevaluation. *Plant Sci 8*:221–229.

Schumacher J, Randles JW, Riesner D. 1983. A two-dimensional electrophoretic technique for the detection of circular viroids and virusoids. *Anal Biochem 135*:288–295.

Semancik JS, ed. 1987. *Viroids and viroid-like pathogens*. Boca Raton, Florida: CRC Press.

Steger H, Hofmann G, Förtsch J, Gross HJ, Randles JW, Sänger HL, Riesner D. 1984. Conformational transitions in viroids and virusoids: Comparison of results from energy minimization algorithm and from experimental data. *J Biomol Struct Dyn 2*:543–571.

Steger G, Tabler M, Brüggemann W, Colpan M, Klotz G, Sänger HL, Riesner D. 1986. Structure of viroid replicative intermediates: Physico-chemical studies on SP6 transcripts of cloned oligomeric potato spindle tuber viroid. *Nucleic Acids Res 14*:9613–9630.

Tsagris M, Tabler M, Sänger HL. 1987. Oligomeric potato spindle tuber viroid RNA does not process autocatalytically under conditions where other RNAs do. *Virology 157*:227–231.

Turner DH, Sugimoto N, Freier SM. 1990. Thermodynamics and kinetics of base-pairing and of DNA and RNA self-assembly and helix coil transition. In: Sänger W, ed. *Nucleic Acids, Subvolume c, Physical Data I, Spectroscopic and Kinetic Data. Landolt-Börnstein, Group VII Biophysics, Vol I.* Berlin, Germany: Springer-Verlag. pp 201–212.